

Reactive Whole-Body Obstacle Avoidance for Collision-Free Human-Robot Interaction with Topological Manifold Learning

Apan Dastider and Mingjie Lin

Abstract—Safe collaboration between human and robots in a common unstructured environment becomes increasingly critical with the emergence of Industry 4.0. However, to accomplish safe, robust, and autonomous collaboration with humans, modern robotic systems must possess not only effective proximity perception but also reactive obstacle avoidance. Unfortunately, for most robotic systems, their shared working environment with human operators may *not* always be static, instead often dynamically varying and being constantly cluttered with unanticipated obstacles or hazards.

In this paper, we present a novel methodology of reactive whole-body obstacle avoidance methodology that safeguards the human who enters the robot’s workspace through achieving conflict-free human-robot interactions even in a dynamically constrained environment. Unlike existing Jacobian-type or geometric approaches, our proposed methodology leverages both topological manifold learning and latest deep learning advances, therefore can not only be readily generalized into other unseen problem settings, but also achieve high computing efficiency with concrete theoretical basis. Furthermore, in sharp contrast to the industrial cobot setting, our methodology allows a robotic arm to proactively avoid obstacles of arbitrary 3D shapes without direct contacting.

To solidify our study, we implement and validate our methodology with a robotic platform consisting of dual 6-DoF robotic arms with optimized proximity sensor placement, both of which are capable of working collaboratively with different levels of interference. Specifically, one arm will perform reactive whole-body obstacle avoidance while achieving its pre-determined objective, with the other arm emulating the presence of a human collaborator with independent and potentially adversary movements. We have showcased the complete video demonstrations of our robotic experiments in this link : <https://sites.google.com/view/roa-a/home>.

Index Terms—Human-Robot Interaction, Obstacle Avoidance, Manifold Learning, Dynamic Constrains

I. INTRODUCTION

The modern environment of cooperative working stipulates human-machine or machine-machine to interact seamlessly [1], [2]. However, to achieve conflict-free collaboration while achieving collective objectives, robotic agents have to satisfy two criteria. First, the working entity, whether a machine or a human worker, must be capable of handling a dynamic working environment with constantly changing obstacles and system constraints [3]. Second, to ensure the timeliness of response, the human or machine agent has to compute an effective control policy that meets a real-time learning performance. To alleviate both challenges, this paper, under a adaptive motion planning algorithm, as shown in Fig. 1, formulates the problem of *Reactive Obstacle Avoidance* (ROA), where one robotic agent (*arm.2*) can dexterously avoids a moving 3D obstacle (*arm.1*) with potentially changing form in real time while achieving its own objective.

Fundamentally, our methodology leverages two key tech-

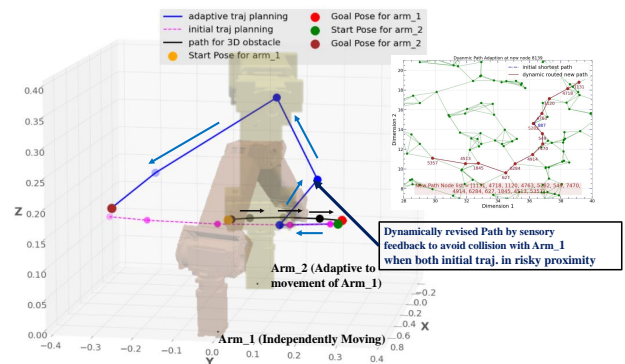


Fig. 1: The reactive path planning from sensory feedbacks to avoid probable collisions with arm.1.

nologies: 1) topological manifold learning and 2) DNN-based deep learning for dimension reduction. Practically, our methodology consists of three key steps. First, we solve a obstacle avoidance problem with an arbitrary but fixed obstacle location and an arbitrary objective. This solution will serve as the basic building block of our overall strategy. Second, we develop a scheme to optimally place vicinity sensors on the robotic surface area, which minimizes the total number of vicinity sensors and maximizes the overall detection coverage. Finally, we construct a novel scheme to dynamically determine the most critical collision point when a given robotic arm interacts with a 3D obstacle subject that not only moves but also potentially changes its form on the fly.

Contributions. We propose integrating *topological manifold learning* with *deep autoencoding* synergistically in order to efficiently generate adaptable motion policy for dynamically constrained environment with unforeseen obstacles. Our paper claims the following contributions:

- 1) Our developed algorithm exploits manifold learning to embed complex system dynamics with low-dimensional space in order to drastically simplify robotic motion planning, whereas most existing whole-body obstacle avoidance algorithms need to fully consider specific problems setting individually.
- 2) Our proposed algorithm can generalize to tackle dynamic variations in objectives and working environment in the presence of obstacles or hazards. In fact, these obstacles can not only dynamically change their shapes but also take arbitrary moving trajectories, therefore providing significant flexibility.
- 3) Unlike most prior work, our study doesn’t assume a global camera in order to detect and localize all obstacles and the pose of robotic manipulator. Instead, we localize all relevant objects using only multiple vicinity sensors strategically placed on the external surface of

our robotic arm.

II. PROBLEM FORMULATION

To formulate our work formally, we conceive two robotic agents *arm_1* and *arm_2* working collaboratively as in Fig. 6, both equipped with independent trajectory planning respectively. It should be noted that trajectory planning only need to be functionally compatible, but not necessarily identical. Furthermore, we assume the robot arm *arm_1* plays a key role for achieving their collective objective, therefore given a prioritized treatment over the agent *arm_2*. As such, *arm_1* will act according to its own planned motion while being oblivious of *arm_2*. However, *arm_2*, being a subordinate, will pay full attention to *arm_1* through receiving sensory feedback. Specifically, during their collaborative interaction, *arm_1*, not intentionally, will dynamically generate motion obstacles against *arm_2*, whereas *arm_2* will constantly modify its prior motion planning as depicted in Fig.1 in order to flawlessly avoid any hurdles from *arm_1*.

III. PROPOSED METHODOLOGY

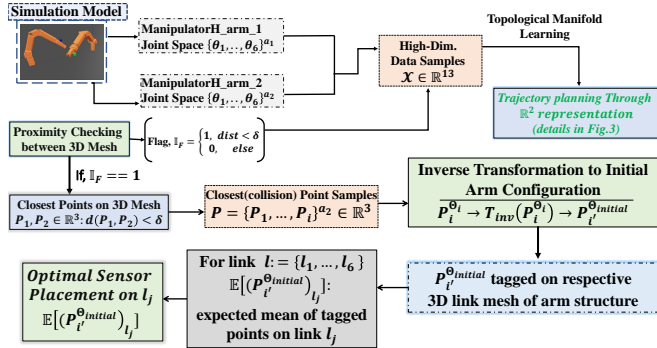


Fig. 2: Algorithmic block diagram of Optimal Sensor Placement Method.

Figure 2 depicts the overall structure of our proposed methodology. It consists of two major algorithm modules: 1) optimal proximity sensor placement such that the robotic manipulator can preemptively sense potential collision with moving unknown obstacles. 2) manifold-based robotic planning to dynamically avoid moving obstacles, which is accomplished with three sub-modules: a) topological manifold learning, which transforms high-dimensional robotic poses into low-dimensional 2D data points in order to facilitate robotic path planning and obstacle avoidance, b) variational autoencoding/decoding, which bridges between high-dimensional robotic poses and low-dimensional manifold spaces, and c) graph construction and traversing, which performs robotic control and obstacle avoidance by traversing and rerouting a 2D sparsely-connect graph efficiently.

Algorithm Block 1: Optimal Proximity Sensor Placement

Proximity perception, central to human-centered robotics, can fulfill the promise of safe, robust, and autonomous systems in industry and daily life, alongside humans. In this study, we place all proximity sensors on the exterior of manipulator arms. We use commercially available acoustic sensors for ranging based ultrasound wave propagation. However, unlike in Fig. 3, we investigate how to optimally place acoustic-based proximity sensors, therefore indirectly minimizing the number of sensors needed. We

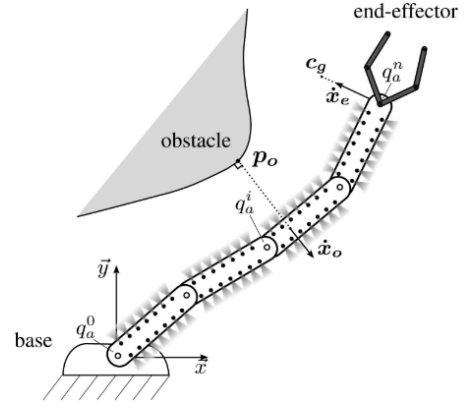


Fig. 3: Redundant robot, equipped with proximity sensors on its links, can move toward a target end-effector configuration, while simultaneously moving some of the links of the robot away from an obstacle. (Figure adapted from [4]).

have accumulated the collision points of both arms from our simulation platform and applied a simple mathematical transformation metric to tag the collision points of robotic arm's 3D collision mesh as shown in Fig.2. To find the collision points of 3D mesh on respective link $l_{\{j=2, \dots, 6\}}$, we are required to inversely transform the collision points from world frame to the respective link frame. For that, we have used following inverse relationship between points lying at different coordinate systems,

$$P_{i^{th} \text{ frame}}^{\Theta_j} = [T_0^1 \dots T_{i-1}^i]^{-1} P_{reference \text{ frame}}^{\Theta_j} \quad (1)$$

where, $T_{i-1}^i = \begin{bmatrix} R_{\theta_{i-1}} & | & Trans_{i-1} \\ \mathbf{0} & | & 1 \end{bmatrix}$. Here, $R_{\theta_{i-1}}$ is rotation angle while moving from $(i-1)^{th}$ coordinate frame to frame i^{th} frame and $Trans_{i-1}$ is the respective translation of origin. Since, the simulation tool only gives access to the coordinate values with respect to world frames, we need to transform the collision coordinates to respective link coordinate frames. It assists us to tag the collision points on the correct position of the 3D mesh of accurate link. Moreover, we have also enforced the algorithm to the reverse rotations for any collisions for traversing back to initial pose from any colliding joint configuration after the dataset is fully collected. Thus, the collision points are also traversed back to initial pose which greatly facilitates to tag the collision point on each arm. Through accumulating a considerable amount of colliding points for each link as well as each plane on the link, we learn a non-uniform distribution over planar co-ordinates for each plane. The expected value $\mathbb{E}[P_x, P_y]$ can be assumed as the optimal proximity sensor location for covering most collision surface.

Algorithm Block 2: Topological Manifold Learning

Manifold learning is a well-known mathematical framework for investigating the geometrical structure of datasets in high-dimensional spaces. In this paper, we consider the high-dimensional space defined by $\{\{\theta_0, \theta_1, \dots, \theta_6\}_{arm.1}; \{\theta_0, \theta_1, \dots, \theta_6\}_{arm.2}; \mathbb{C}_F\}$, where $\{\theta_i\}_{arm.i}$ s determine the exact full-pose end-effector trajectory of robotic arm $i \in \{1, 2\}$ and \mathbb{I}_F is the collision flag. Our crucial insight is that the geometrical structure of our considered high-dimensional space incorporates the

complex system dynamic between full pose of both robotic arms for arbitrary joint configurations. In order fully extract and leverage the embedding power of our learned manifold, we perform a dimension reduction with the well-known isometric embedding [5] from high-dimensional robotic space to the low-dimensional manifold space that can be more readily be computed for robotic motion planning. It is important to note that all these dimension reductions are done under the condition that the metric tensor is preserved between these two spaces.

Algorithm Block 3: Variational Autoencoding/Decoding

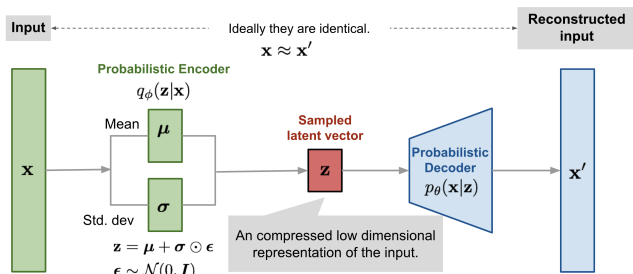


Fig. 4: Schematic of a variational autoencoder.

To facilitate our manifold-based robotic motion planning, we need to seamlessly transform between high-dimensional robotic space \mathcal{R} and low-dimensional mathematical space \mathcal{M} . For this, we use a well-established deep learning technique: variational autoencoder (VAE) [6]. Conceptually, an autoencoder consists of both an encoder and a decoder. In fact, autoencoders are typically forced to reconstruct the input approximately, preserving only the most relevant aspects of the data in the copy. In our study, we implement autoencoders as deep neural networks in order to perform dimensionality reduction only. Specifically, our autoencoder is implemented as a feedforward, non-recurrent neural network employing an input layer and an output layer connected by one or more hidden layers. The output layer has the same number of nodes (neurons) as the input layer. The purpose of our autoencoder is to reconstruct its inputs (minimizing the difference between the input and the output) instead of predicting a target value \mathbf{Y} given inputs \mathbf{X} .

Our autoencoder consists of two parts, the encoder and the decoder, which can be defined as transformations ϕ and ψ , such that: $\phi : \mathcal{X} \rightarrow \mathcal{F}$ and $\phi : \mathcal{F} \rightarrow \mathcal{X}$ and $\phi, \psi = \arg \min \|\mathcal{X} - (\psi \circ \phi)\mathcal{X}\|^2$. Autoencoders are trained to minimise reconstruction errors (such as squared errors), often referred to as the “loss” $\mathcal{L}(\mathbf{x}, \mathbf{x}') = \|\mathbf{x} - \mathbf{x}'\|^2$, where \mathbf{x} is usually averaged over the training set. Our autoencoder is trained through backpropagation of the error. Conceptually, the feature space \mathcal{F} of our autoencoder is the low-dimension manifold representations produced by manifold learning, therefore having lower dimensionality than the input space \mathcal{X} , which, in our study, is the pose of our 7-DoF robotic manipulator. As such, the feature vector $\phi(x)$ after manifold learning can be regarded as a compressed representation of the input x .

Algorithm Block 4: Graph Construction and Traversing

Graph-based robotic motion planning has been well established [7], however mostly applied in the arena of mobile

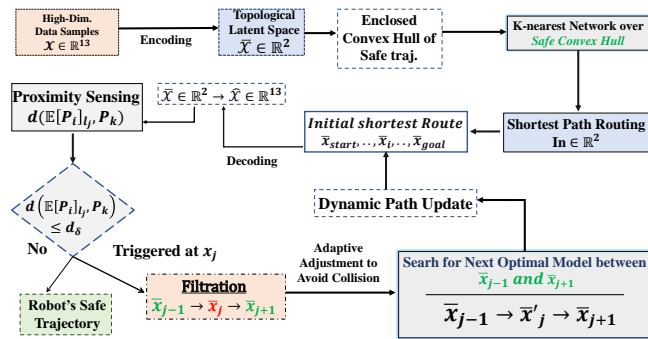


Fig. 5: Block Diagram of Trajectory Planning Through Manifold Space

robots navigating in complex environments. In this, the graph we construct the system dynamic between robotic manipulator and the adversarial 3D moving mesh i.e another robotic arm through a topological manifold space. In our study, we choose to use 2D for our low-dimensional manifold space to simplify our graph data structure and its traversing. Specifically, after our manifold space is created, we will have a set of 2D vertices labelled either as “collision” or “collision free”. During our robotic arm motion planning, we will perform shortest-distance routing using the well-known Dijkstra’s algorithm with only the green vertices (“collision-free”). The graph internal data structures of our 2D graph are based on an adjacency list representation and implemented using Python dictionary data structures. Furthermore, the graph adjacency structure is implemented as a Python dictionary of dictionaries; the outer dictionary is keyed by nodes to values that are themselves dictionaries keyed by neighboring node to the edge attributes associated with that edge. This “dict-of-dicts” structure allows fast addition, deletion, and lookup of nodes and neighbors in large graphs. All of our functions manipulate graph-like objects solely via predefined API methods and not by acting directly on the data structure. Our software code is largely based on the open-source NetworkX package [8].

IV. SYSTEM OVERVIEW

A. Experimental Platform and Simulation Setup

As shown in Fig.6, we used here two research-grade 6-DOF robotic manipulators of Robotis® Manipulator-H, *arm_1* and *arm_2*, that are mounted on a grid mapped tabletop which served as a shared and concise workspace for all experiments. We have installed a 400×600 resolution touch-sensitive frame to locate the target positions for both arms. Specifically, *arm_1* serves the purpose of creating dynamic occlusions while maneuvering for the adaptive robotic agent *arm_2*. The adaptive planning algorithm runs on a Lambda QUAD GPU workstation equipped with Intel Core-i9-9820X (10 cores) processor and Ubuntu 18.04. Moreover, the adaptive entity *arm_2* is empowered with proximity sensors embodied at optimal location for accurate collision detection followed by adaptive route traversing. The feedback of these sensors are recorded through a Raspberry PI to the controller. Our mechanical platform is integrated with PID values to introduce precise position control [9] within safe range.

On the other hand, to replicate the hardware setup in order to accumulate dataset and validate our approach, we have

created high-fidelity robot models inside Robotics Toolbox for Python [10] which has been very recently forked out of its older version well-known for Matlab. With the open-sourced robot description files—URDF files, we easily replicated the models inside the simulated environment and we exploited the available functionalities for checking collision among 3D meshes or tagging proximal points among 3D meshes in the simulation. For establishing the inter-processing communication (IPC) protocol to ensure low-latency data processing and parallel execution among simulation environments and real hardware, we have encapsulated the framework inside the Robot Operating System (ROS) ecosystem.

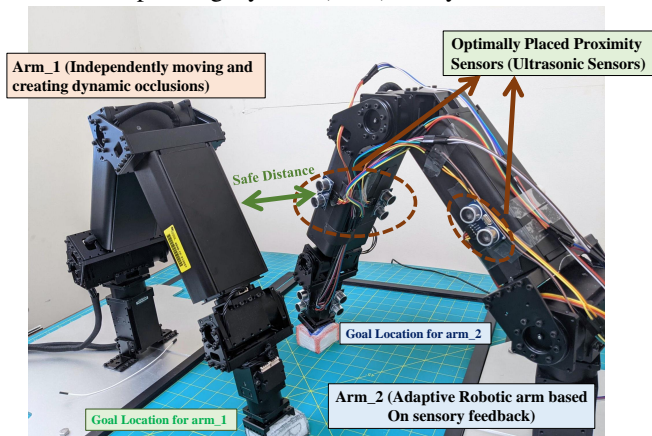


Fig. 6: Hardware Platform with Sensor Attachment

B. Experimental Procedures and Learning Variables

We now define key variables in high-dimensional data for building the latent space manifold representation. The dataset comprises 27 variables—6x2 joint angles $\{\theta_i^a\}_{i=0,\dots,5}^{a=1,2}$, 7x2 pose variables containing quaternion orientations in $\mathbb{R}^3 \times \mathcal{S}^3$ and binary collision flag, \mathbb{C}_F . Besides, to optimally allocate the proximity sensors on different links $\{l_i\}_{i=2,\dots,6}$ of *arm_2*, we also logged the closest point coordinates with link IDs on 3-D meshes while colliding. Since, base link is fixed and out of the confined workspace, it is unnecessary to tag collision points on it. The control command Θ_i^a for each arm is a vector of 6 joint angles. Since, data accumulation process is very stochastic in nature and both robotic arms can collide with each other for multiple instances, we used the simulation platform for dataset collection and initial learning purposes. When the algorithm and manifold construction converges, the validation experiments are carried over varying goal locations and random occlusions created by *arm_1* in real hardware setup for real-time and scalable applications of our algorithms. Our VAE architecture is implemented on Pytorch [11]. The decoder and encoder network comprises on three layers with $\{450, 250, 100\}$ neurons. The encoded latent space representation lies in \mathbb{R}^2 which greatly facilitates creating graph embedding to plan optimal path from node to node. Notably, the 3D occlusions created here by *arm_1* can be easily substituted by any 3D structures which confirms that our method can be easily extended to a safe and optimal robot-robot and human-robot collaborative framework.

V. RESULTS ANALYSIS

Our experiments seek to investigate the following:

- 1) Can we create a resolution to optimal sensor placement

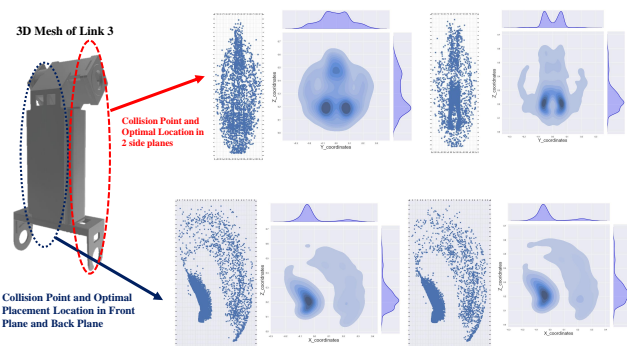


Fig. 7: Collision points on link 3 and Optimal sensor placement location calculated through non uniform distributions

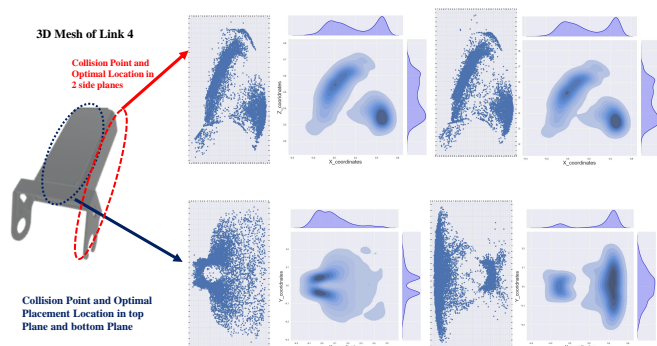


Fig. 8: Collision points on link 4 and Optimal sensor placement location calculated through non uniform distributions

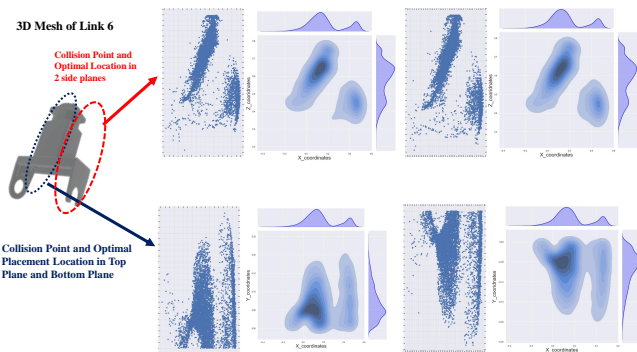


Fig. 9: Collision points on link 6 and Optimal sensor placement location calculated through non uniform distributions problem through tagging the colliding points to respective links and creating the non-uniform distributions over coordinate values for each plane of cuboid links?

- 2) Can we learn two disparate convex hulls in \mathbb{R}^2 space representing the safe and colliding samples for initial feasible trajectory?
- 3) Can we concurrently handle the unseen perturbations and adaptively re-plan trajectory over *safe* convex hull to reach the goal location?

A. Ideal and Efficient Sensor Placement

In this work, we attempted to address the issue of positioning the proximity sensors optimally on mechanical structure of the different links. To solve the task of maneuvering inside a concise workspace, sensors should be embodied on

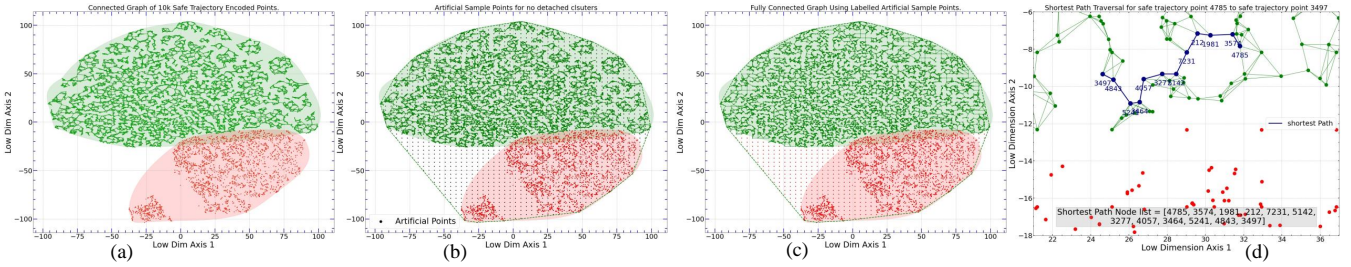


Fig. 10: (a) Connected Network over 10k Manifold Points, (b)-(c) Uniformly Sampled Points for a densely Connected

Network, (d) Shortest Path Routing by Dijkstra's algorithm such locations which appeared to be high probable colliding surface on robot structure. To resolve this issue, our data samples contain the location of closest points in \mathbb{R}^3 space on the collision meshes of adaptive robotic arm. Through applying inverse transformation matrix shown in Section II and inverse rotation to the initial pose from Θ^j of the robot arm, we tag this collision points on the initial pose of mechanical structure of robotic arm. In Fig. 78,9, we showed the optimal sensor positions for 4 different planes of 3 longest links of Manipulator-H robotic arm. The joint plots are depicted based on coordinate values from respective planes of links when robot is spawned at its initial locations. The estimated distributions from the independent variables manifests the high probable location of collisions and sensors should be embodied on such points to gain effective collision avoidance feedback from proximity sensors. For instance, the top plane of Link 6 spawns parallelly to XY plane and only $\{P_{x_j}, P_{y_j}\}_{l_6}$ collision coordinates are used to manifest the distributions. As mentioned in the methodology section, the mean value $\mathbb{E}[P_{x_j}, P_{y_j}]$ are assumed to be the optimal sensor placement locations on top plane of link 6 for having the most efficient collision avoidance feedback for dynamically re-planning to assure safe trajectory. Fig. 7,8,9 manifests the most systematic sensor placement locations for significant and longest links of our adaptive manipulator.

B. Latent Space Representation and Routing over Graphs

Each data sample comprises the joint angle values from both arms as well as a collision flag C_F which is either 0 when collided or 1 when a safe trajectory is finished. With this high-dimensional representation, our VAE learns a topological manifold representation in \mathbb{R}^2 . As shown in Fig.11, the latent space manifold sample points can be smoothly differentiated between two clusters of safe trajectory and colliding trajectory. Although there persists a narrow overlapping space between two convex hulls, still it is promisingly apparent that the sample representation remains distinct in \mathbb{R}^2 space as well. The collision indicator flag and inter-relationship between synchronously sampled joint space poses for safe trajectories and colliding trajectories enable the algorithm to effectively learn these disparate manifold representation through variational encoding. On the next step, we moved forward to create a connected graph over only the space encompassing the successful trajectories which has been shadowed with green color in Fig.11. By incorporating unsupervised K-Nearest neighboring algorithm for connecting to neighboring vertices in the safe manifold space, we created here a connected graph network which facilitates shortest path routing from any vertice as start pose

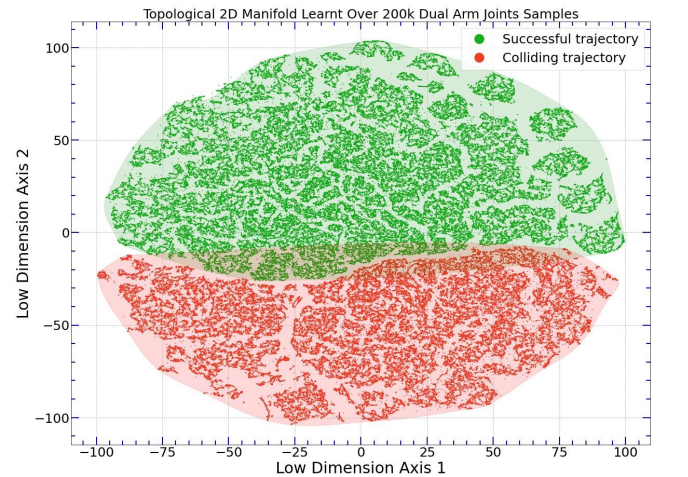


Fig. 11: Two separate convex hulls

and another vertice as goal position for adaptive robotic agent. As shown in Fig.10(a), while creating connected graphs, sub-clusters are created automatically inside the safe manifold. This generation of disparate sub-clusters violates highly the notion of complete path routing from any random to another random node on the connected network. To confirm a dense connection, we artificially sample points in same \mathbb{R}^2 space as grid mesh over the convex hulls. With our trained decoder part of VAE, we can tag these artificial points as safe/colliding trajectories which is shown if Fig.10(c). From the similarity of labels of classified points between Fig.11 and Fig.10(c), it is also confirmed that global structure of the manifold space is successfully maintained through Variational Encoding. Now, we obtained a densely connected network over all green points which guarantees that our first initial routed path can be presumed to be a safer trajectory. To route the shortest path, we have utilized here a very well-known shortest routing algorithm over connected networks Dijkstra's algorithm here.

C. Dynamic Obstacle Avoidance

The main goal of our research work is to devise a method established on 2-D manifold representation for concurrently avoiding dynamic obstacles created by another robotic arm arm_1 and re-planning its trajectory to reach goal position within shortest possible time. Since, the networks over the safe low-dimensional points are densely connected and our algorithm makes sure there exists at least one connecting edge between any two random nodes, it is effortlessly plausible to perturb the initial route and form a new route by changing the intermediate node and edge connections. Whenever the adaptive entity encounters an occlusion while

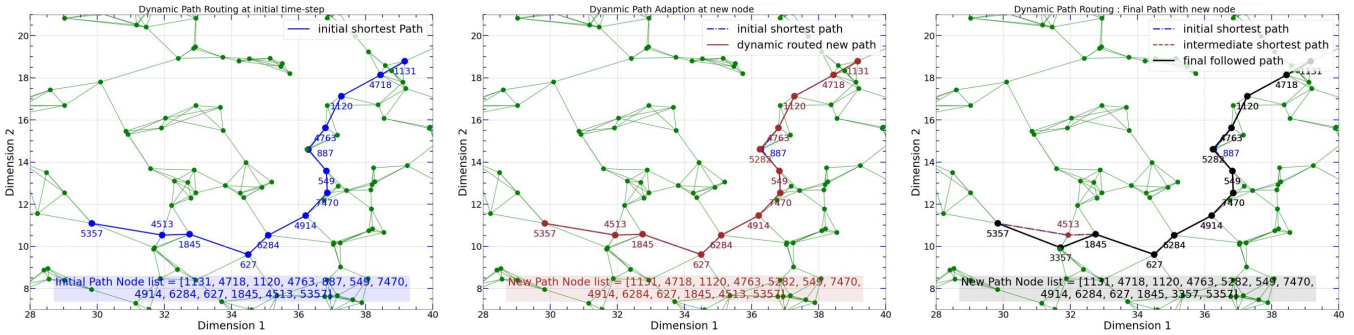


Fig. 12: Dynamic Path routing for avoiding collision: (a) Initial Sampled Path (b) Path Change for avoiding first perturbation (c) Comparison of final followed path and initial path

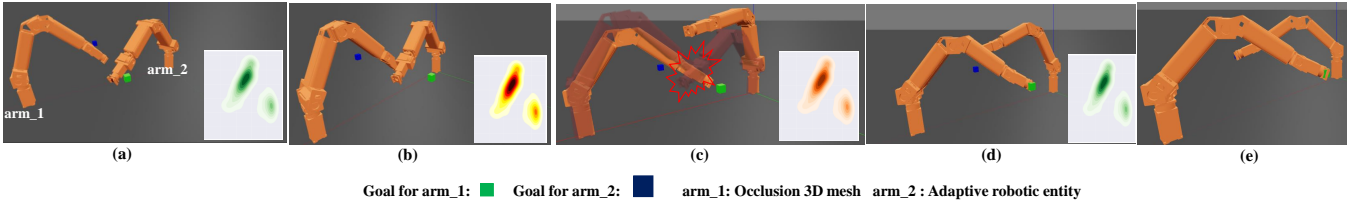


Fig. 13: Dynamic Trajectory Planning: (a) Initial Pose (b) Both arms on verge of collision—sensors triggered (c) adaptive *arm_2* re-routes through new node and adapts new trajectory to avoid collision—sensors feedback slightly changes (d) both arms following safe trajectory—feedback neutralises

following its initial trajectory, it receives a sensory feedback of possible collision and avoids following the colliding nodes. Instead the algorithm enables the robotic arm to re-plan the shortest path through the next best shortest path. Thus, the adaptive learner dynamically avoids the obstacle in between travelling to goal pose from the initial pose. This idea has been drawn in Fig.12 where the initial routing has adaptively modified at two different time-steps based on negative(collision) sensory feedback from the proximity sensors. Moreover, the decoder part of the VAE is employed to get joint poses for these selected manifold points.

In Fig. 13, we have included snapshots of optimized and adaptive trajectory planning in a framework of robot-robot interaction when both arms have to maneuver in a concise workspace. In Fig.13(b), whenever both robotic manipulators are in very close proximity and heading to a possible catastrophe, the proximity sensors embodied in robot body are triggered and controller receives feedback to stop current trajectory and modify the initial shortest path. The negatively triggered feedback is shown through red colormap in the Fig.13(b). In the next snapshot (c), we noticed that the *arm_2* has concurrently changes its initial path to avoid a collision. In this part, we also included in red shaded image of how both arms will collide if no dynamic re-routing is engaged in our approach. Also, sensory feedback changes positively as the proximal distance between two robotic entity enhances. Here, path adaptation happens only on single node to avoid dynamic obstacles, so our algorithm also achieve an optimized trajectory planning and execution. In Fig.13 (d) and (e), it is clearly seen that both robotic manipulators have reached to their goal positions smoothly and safely.

VI. CONCLUSION

Our research aims at developmentally or continuously constructing robotic policy against dynamically generated obsta-

cles or state constraints. Our key idea is to synergistically integrate optimally placed proximity sensors that preemptively sense dynamic obstacles with a reactive robotic motion planning algorithm based on topological manifold learning, variational autoencoder, and incremental graph traversal. We believe that our proposed algorithm can be widely useful in many empirical settings, especially when global scene camera is absent and algorithm reuse is paramount.

REFERENCES

- [1] M. A. Goodrich and A. C. Schultz, “Human-robot interaction: A survey,” *Foundations and Trends in Human-Computer Interaction*, vol. 1, no. 3, pp. 203–275, 2007.
- [2] P. S. Schmitt, F. Witnshofer, K. M. Wurm, G. V. Wichert, and W. Burgard, “Modeling and planning manipulation in dynamic environments,” *Proceedings - IEEE International Conference on Robotics and Automation*, vol. 2019-May, pp. 176–182, 2019.
- [3] P. S. Schmitt, F. Wirnshofer, K. M. Wurm, G. v. Wichert, and W. Burgard, “Planning reactive manipulation in dynamic environments,” in *2019 IEEE/RSJ International Conference on Intelligent Robots and Systems (IROS)*. IEEE, 2019, pp. 136–143.
- [4] A. Maciejewski and C. Klein, “Obstacle avoidance for kinematically redundant manipulators in dynamically varying environments,” *The International Journal of Robotics Research*, vol. 4, 09 1985.
- [5] A. H. Khan, S. Li, and X. Luo, “Obstacle Avoidance and Tracking Control of Redundant Robotic Manipulator: An RNN-Based Metaheuristic Approach,” *IEEE Transactions on Industrial Informatics*, vol. 16, no. 7, pp. 4670–4680, 2020.
- [6] D. P. Kingma and M. Welling, “Auto-encoding variational bayes,” 2014.
- [7] T. Dang, F. Mascarich, S. Khattak, C. Papachristos, and K. Alexis, “Graph-based path planning for autonomous robotic exploration in subterranean environments,” in *2019 IEEE/RSJ International Conference on Intelligent Robots and Systems (IROS)*, 2019, pp. 3105–3112.
- [8] A. A. Hagberg, D. A. Schult, and P. J. Swart, “Exploring network structure, dynamics, and function using networkx,” in *Proceedings of the 7th Python in Science Conference*, G. Varoquaux, T. Vaught, and J. Millman, Eds., Pasadena, CA USA, 2008, pp. 11 – 15.
- [9] K. Ota, D. K. Jha, T. Oiki, M. Miura, T. Nammoto, D. Nikovski, and T. Mariyama, “Trajectory Optimization for Unknown Constrained Systems using Reinforcement Learning,” pp. 3487–3494, 2019. [Online]. Available: <http://arxiv.org/abs/1903.05751>
- [10] P. Corke and J. Haviland, “Not your grandmother’s toolbox – the robotics toolbox reinvented for python,” in *2021 IEEE International*

Conference on Robotics and Automation (ICRA), 2021, pp. 11 357–11 363.

- [11] A. Paszke, S. Gross, F. Massa, A. Lerer, J. Bradbury, G. Chanan, T. Killeen, Z. Lin, N. Gimelshein, L. Antiga, A. Desmaison, A. Kopf, E. Yang, Z. DeVito, M. Raison, A. Tejani, S. Chilamkurthy, B. Steiner, L. Fang, J. Bai, and S. Chintala, “Pytorch: An imperative style, high-performance deep learning library,” in *Advances in Neural Information Processing Systems* 32, H. Wallach, H. Larochelle, A. Beygelzimer, F. d’Alché-Buc, E. Fox, and R. Garnett, Eds. Curran Associates, Inc., 2019, pp. 8024–8035. [Online]. Available: <http://papers.neurips.cc/paper/9015-pytorch-an-imperative-style-high-performance-deep-learning-library.pdf>